# An inverse problem of finding the time-dependent diffusion coefficient from an integral condition

M.S. Hussein[1,2], D. Lesnic[1] and M.I. Ismailov[3]
[1]*Department of Applied Mathematics, University of Leeds, Leeds LS2 9JT, UK*
[2]*Department of Mathematics, College of Science, University of Baghdad, Baghdad, Iraq*
[3]*Department of Mathematics, Gebze Institute of Technology, Gebze-Kocaeli 41400, Turkey*
E-mails: mmmsh@leeds.ac.uk (M.S. Hussein), amt5ld@maths.leeds.ac.uk (D. Lesnic), mismailov@gyte.edu.tr (M.I. Ismailov).

**Abstract**
We consider the inverse problem of determining the time-dependent diffusivity in the one-dimensional heat equation with periodic boundary conditions and nonlocal over-specified data. The problem is highly nonlinear and it serves as a mathematical model for the technological process of external guttering applied in cleaning admixtures from silicon chips. First, the well-posedness conditions for the existence, uniqueness and continuous dependence upon the data of the classical solution of the problem are established. Then, the problem is discretised using the finite-difference method and recast as a nonlinear least-squares minimization problem with a simple positivity lower bound on the unknown diffusivity. Numerically, this is effectively solved using the *lsqnonlin* routine from the MATLAB toolbox. In order to investigate the accuracy, stability and robustness of the numerical method, results for a few test examples are presented and discussed.

**Keywords:** Inverse problem; Thermal diffusivity; Integral condition.

# 1 Introduction

Parameter identification from over-specified data plays an important role in applied mathematics, physics and engineering. The problem of identifying the diffusivity was investigated by many researchers under various boundary and overdetermination conditions, [5–8, 14]. It is important to note that in [12], the time-dependent diffusion coefficient has been determined from different over-determination conditions in the case of self-adjoint auxiliary spectral problems.

In the present work, a nonlocal over-specified data is used together with periodic boundary conditions for the determination of the time-dependent diffusivity. The mathematical formulation of the inverse problem under investigation is given in Section 2. In Section 3, the existence, uniqueness and continuous dependence upon the data of the classical solution of the inverse problem for some small parameters are established by using the generalized Fourier method. The numerical methods for solving the direct and inverse problems are described in Sections 4 and 5, respectively. Numerical results are presented in Section 6. Finally, conclusions are highlighted in Section 7.

# 2 Mathematical Formulation

In the rectangle $Q_T = \{(x,t)|\, 0 < x < 1,\, 0 < t \leq T\} = (0,1) \times (0,T]$, we consider the inverse problem given by the heat equation

$$\frac{\partial u}{\partial t}(x,t) = k(t)\frac{\partial^2 u}{\partial x^2}(x,t), \qquad (x,t) \in Q_T, \tag{1}$$

with unknown concentration/temperature $u(x,t)$ and unknown time-dependent diffusivity $k(t) > 0$, subject to the initial condition

$$u(x,0) = \varphi(x), \qquad 0 \leq x \leq 1, \tag{2}$$

where $\varphi$ is a given function, the periodic and heat flux boundary conditions

$$u(0,t) = u(1,t), \qquad t \in (0,T], \tag{3}$$

$$u_x(1,t) = 0, \qquad t \in (0,T], \tag{4}$$

and the over-determination condition, [9, 10],

$$p(t)u(0,t) + \int_0^1 u(x,t)dx = E(t), \qquad t \in [0,T], \tag{5}$$

with $p(t) = \alpha + \beta k^{-\gamma}(t)$, where $\alpha$, $\beta$, $\gamma > 0$ are segregation coefficients. This problem arises in the mathematical modelling of the technological process of external guttering applied, for example, in cleaning admixtures from silicon chips, [10]. In this case, $\varphi(x)$ is the distribution of admixture in the chip for $x \in (0,1)$ at the initial time $t = 0$, while $u(x,t)$ is its distribution at time $t$. Condition (3) means that the admixtures in the left and right boundaries of the chip are the same. The adiabatic condition (4) means that the right boundary $x = 1$ of the chip is perfectly insulated. Condition (5) means that part of the substance is concentrated (segregated) on the left side $x = 0$ of the chip, [9, 10].

When $\alpha = \beta = 0$ then, the resulting inverse problem has been previously investigated in [5], and it is the purpose of this paper to investigate the non-trivial case when $\alpha$ and $\beta$ are non-zero.

# 3 Mathematical Analysis

## 3.1 Existence and Uniqueness

The pair $(k(t), u(x,t))$ from the class $C[0,T] \times \left(C^{2,1}(Q_T) \cap C^{1,0}\left(\overline{Q}_T\right)\right)$ for which conditions (1)-(5) are satisfied and $k(t) > 0$ on the interval $[0,T]$, is called the classical solution of the inverse problem (1)-(5).

The analysis is similar to that of [4] for the identification of the time-dependent blood perfusion coefficient in the bio-heat equation. Consider the spectral problem

$$X''(x) + \lambda X(x) = 0, \quad 0 \leq x \leq 1, \tag{6}$$

$$X(0) = X(1), \quad X'(1) = 0. \tag{7}$$

This problem is well-known in [3], as the auxiliary spectral problem for solving a nonlocal boundary value problem for heat equation by the Fourier method.

It is easy to show that the problem (6) and (7) has the eigenvalues

$$\lambda_n = (2\pi n)^2, \quad n = 0, 1, 2, ...$$

and the system of eigenfunctions and associated functions

$$X_0(x) = 2, \quad X_{2n-1}(x) = 4\cos(2\pi nx), \quad X_{2n}(x) = 4(1-x)\sin(2\pi nx), \quad n = 1, 2, ... \quad (8)$$

The system of functions $X_n(x)$, $n = 0, 1, 2, ...$ is a basis in $L_2[0, 1]$, [3].

The adjoint problem to (6) and (7) has the form

$$Y''(x) + \lambda Y(x) = 0, \quad 0 \le x \le 1, \quad (9)$$

$$Y(0) = 0, \quad Y'(0) = Y'(1). \quad (10)$$

Analogously to the problem (6) and (7), the system of eigenfunctions and associated functions of the problem (9) and (10) is given by

$$Y_0(x) = x, \quad Y_{2n-1}(x) = x\cos(2\pi nx), \quad Y_{2n}(x) = \sin(2\pi nx), \quad n = 1, 2, .... \quad (11)$$

It is easy to show that the systems (8) and (11) form a bi-orthonormal system on the interval $[0, 1]$, i.e.

$$(X_i, Y_j) = \int_0^1 X_i(x)Y_j(x)dx = \delta_{ij},$$

where $\delta_{ij}$ is the Kronecker delta tensor.

The following lemmas are important for the mathematical analysis of the inverse problem.

**Lemma 1.** *If $\phi(x) \in C^3[0, 1]$ satisfies the conditions $\phi(0) = \phi(1)$, $\phi'(1) = 0$, $\phi''(0) = \phi''(1)$ then the inequalities*

$$\sum_{n=1}^{\infty} n^2 |\phi_{2n}| \le c_1 \|\phi\|_{C^3[0,1]}, \quad \sum_{n=1}^{\infty} n |\phi_{2n-1}| \le c_2 \|\phi\|_{C^3[0,1]}, \quad (12)$$

*($c_1$ and $c_2$ are constants)*

*hold, where $\phi_n = \int_0^1 \phi(x)Y_n(x)dx$.*

*Proof.* Because $\phi(0) = \phi(1)$, $\phi''(0) = \phi''(1)$, the equality

$$\phi_{2n} = \int_0^1 \phi(x)\sin(2\pi nx)\,dx = -\frac{1}{8\pi^3 n^3}\int_0^1 \phi'''(x)\cos(2\pi nx)\,dx$$

holds by three times integrating by parts. Analogously, by integrating by parts twice and using that $\phi(0) = \phi(1)$, $\phi'(1) = 0$ we obtain that

$\phi_{2n-1} = \int_0^1 \phi(x)x\cos(2\pi nx)\,dx = -\frac{1}{4\pi^2 n^2}\int_0^1 [x\phi''(x) + 2\phi'(x)]\cos(2\pi nx)\,dx.$

From the above, by using the Schwarz and Bessel inequalities we obtain

$$\sum_{n=1}^{\infty} n^2 \left|\phi_{2n}\right| \leq \frac{1}{8\pi^3} \left[\sum_{n=1}^{\infty} \frac{1}{n^2}\right]^{\frac{1}{2}} \left[\sum_{n=1}^{\infty} \left(\int_0^1 \phi'''(x) \cos\left(2\pi n x\right) dx\right)^2\right]^{\frac{1}{2}}$$
$$\leq c_1 \left\|\phi'''\right\|_{L_2[0,1]} \leq c_1 \left\|\phi\right\|_{C^3[0,1]}$$

and

$$\sum_{n=1}^{\infty} n \left|\phi_{2n-1}\right| \leq \frac{1}{4\pi^2} \left[\sum_{n=1}^{\infty} \frac{1}{n^2}\right]^{\frac{1}{2}} \left[\sum_{n=1}^{\infty} \left(\int_0^1 \left[x\phi''(x) + 2\phi'(x)\right] \cos\left(2\pi n x\right) dx\right)^2\right]^{\frac{1}{2}}$$
$$\leq \frac{c_2}{2} \left\|x\phi'' + 2\phi'\right\|_{L_2[0,1]} \leq c_2 \left\|\phi\right\|_{C^3[0,1]}$$

for some constants $c_1$ and $c_2$. □

**Lemma 2.** *If $k_m(t) \in C\left[0,T\right]$ satisfies the condition $0 < a \leq k_m(t)$, $m = 1,2$ then for $\forall n \in \mathbb{N}$ and $\forall t \in [0,T]$ the inequality*

$$\left|e^{-n\int_0^t k_1(s)ds} - e^{-n\int_0^t k_2(s)ds}\right| \leq \frac{1}{ae} \left\|k_1 - k_2\right\|_{C[0,T]}, \tag{13}$$

*holds.*

*Proof.* For arbitrary fixed $t \in [0,T]$ and $n \in \mathbb{N}$, by using the mean value theorem for the function $e^{-x}$ we obtain that there exists $\theta$ between $n\int_0^t k_1(s)ds$ and $n\int_0^t k_2(s)ds$ such that

$$\left|e^{-n\int_0^t k_1(s)ds} - e^{-n\int_0^t k_2(s)ds}\right| = e^{-\theta} \left|n\int_0^t k_1(s)ds - n\int_0^t k_2(s)ds\right|.$$

By using that $xe^{-bx} \leq \frac{1}{be}$; $x \geq 0$, $b = const. > 0$, we obtain that

$$ne^{-\theta} \left|\int_0^t (k_1(s) - k_2(s))ds\right| \leq e^{-nat} nt \left\|k_1 - k_2\right\|_{C[0,T]} \leq \frac{1}{ae} \left\|k_1 - k_2\right\|_{C[0,T]},$$

and this proves (13). □

The main result of subsection 3.1 is in the following theorem.

**Theorem 1.** *Let the functions $\varphi(x) \in C^3\left[0,1\right]$, $E(t) \in C\left[0,T\right]$ satisfy the conditions*

$$\varphi(0) = \varphi(1),\ \varphi'(1) = 0,\ \varphi''(0) = \varphi''(1), \tag{14a}$$
$$\varphi_{2k} \geq 0,\ \varphi_{2k-1} \leq 0,\ k = 1,2,...,\ \varphi_0 + 2\varphi_1 < 0,\ E(t) < 2\varphi_0, \forall t \in [0,T], \tag{14b}$$

*where $\varphi_n = \int_0^1 \varphi(x) Y_n(x) dx$ for $n = 0,1,2,\cdots$. Then, there exist positive numbers $\alpha_0$ and $\gamma_0$ such that the inverse problem (1)-(5) with the parameters $\alpha < \alpha_0$ , $\gamma > \gamma_0$ has a unique solution, where the numbers $\alpha_0$ and $\gamma_0$ are determined by the data of the problem.*

*Proof.* For arbitrary positive $k(t) \in C[0,T]$, using that $\varphi \in C^3[0,1]$ satisfies the conditions (14a), by applying the standard procedure of the Fourier series method we obtain the solution of the direct problem (1)-(4) in the following form:

$$u(x,t) = \varphi_0 X_0(x) + \sum_{n=1}^{\infty} \varphi_{2n} e^{-(2\pi n)^2 \int_0^t k(s)ds} X_{2n}(x)$$
$$+ \sum_{n=1}^{\infty} \left(\varphi_{2n-1} - 4\pi n \varphi_{2n} t\right) e^{-(2\pi n)^2 \int_0^t k(s)ds} X_{2n-1}(x). \tag{15}$$

The series in (15) and its $x-$partial derivative are uniformly convergent in $\bar{Q}_T$ since their majorizing sums are absolutely convergent by Lemma 1. Therefore, their sums involved in expressing $u(x,t)$ and $u_x(x,t)$ are continuous in $\bar{Q}_T$. Because the majorizing sum $\sum\limits_{n=1}^{\infty} n^3 e^{-K(2\pi n)^2 \varepsilon}$ $(K = const. > 0)$ is convergent, the $t-$partial derivative and the $xx-$second-order partial derivative series of (15) are uniformly convergent for $t \geq \varepsilon > 0$ ($\varepsilon$ is an arbitrary positive number). Thus, we have $u(x,t) \in C^{2,1}(Q_T) \cap C^{1,0}\left(\bar{Q}_T\right)$ which satisfies conditions (1)–(4) for arbitrary positive $k(t) \in C[0,T]$.

Applying the over-determination condition (5), we obtain

$$p(t) = F[p(t)], \tag{16}$$

where

$$F[p(t)] = \frac{2\varphi_0 + \frac{2}{\pi} \sum\limits_{n=1}^{\infty} \frac{1}{n} \varphi_{2n} e^{-(2\pi n)^2 \int_0^t k(s)ds} - E(t)}{-2\varphi_0 + 4 \sum\limits_{n=1}^{\infty} \left[4\pi n \varphi_{2n} t - \varphi_{2n-1}\right] e^{-(2\pi n)^2 \int_0^t k(s)ds}},$$
$$k(t) = \left[\frac{\beta}{p(t) - \alpha}\right]^{\frac{1}{\gamma}}. \tag{17}$$

Denote

$$\alpha_0 = \frac{2\varphi_0 - E_{\max}}{-2\varphi_0 + 4 \sum\limits_{n=1}^{\infty} \left(4\pi n \varphi_{2n} T - \varphi_{2n-1}\right)}, \quad \alpha_1 = \frac{2\varphi_0 + \frac{2}{\pi} \sum\limits_{n=1}^{\infty} \frac{1}{n} \varphi_{2n} - E_{\min}}{-2\varphi_0 - 4\varphi_1}, \tag{18}$$

where $E_{\max} = \max\limits_{t \in [0,T]} E(t)$, $E_{\min} = \min\limits_{t \in [0,T]} E(t)$. Then, from (14b), (16) and (17) it follows that

$$0 < \alpha_0 \leq p(t) \leq \alpha_1, \quad t \in [0,T]. \tag{19}$$

Under condition $\alpha_0 > \alpha$, the inequalities

$$0 < \left[\frac{\beta}{\alpha_1 - \alpha}\right]^{\frac{1}{\gamma}} \leq k(t) \leq \left[\frac{\beta}{\alpha_0 - \alpha}\right]^{\frac{1}{\gamma}} \tag{20}$$

hold.

Let us denote

$$C_{\alpha_0,\alpha_1}[0,T] := \{p(t) \in C[0,T] | \alpha_0 \leq p(t) \leq \alpha_1, \forall\, t \in [0,T]\}.$$

It is easy to verify that

$$F : C_{\alpha_0,\alpha_1}[0,T] \to C_{\alpha_0,\alpha_1}[0,T].$$

Let us show that $F$ is a contraction mapping in $C_{\alpha_0,\alpha_1}[0,T]$, for small $\alpha$ and large $\gamma$. Indeed, $\forall p_1(t), p_2(t) \in C_{\alpha_0,\alpha_1}[0,T]$ we have

$$F[p_1(t)] - F[p_2(t)] = \frac{1}{-2\varphi_0+\alpha_{1,2}(t)} \left( \frac{2\varphi_0+\alpha_{0,1}(t)-E(t)}{-2\varphi_0+\alpha_{1,1}(t)} (\alpha_{1,2}(t) - \alpha_{1,1}(t)) - (\alpha_{0,2}(t) - \alpha_{0,1}(t)) \right), \tag{21}$$

where

$$\begin{aligned} \alpha_{0,m}(t) &= \frac{2}{\pi} \sum_{n=1}^{\infty} \frac{1}{n} \varphi_{2n} e^{-(2\pi n)^2 \int_0^t k_m(s)ds}, \\ \alpha_{1,m}(t) &= 4 \sum_{n=1}^{\infty} (4\pi n \varphi_{2n} t - \varphi_{2n-1})\, e^{-(2\pi n)^2 \int_0^t k_m(s)ds}, \\ k_m &= \left[ \frac{\beta}{p_m(t) - \alpha} \right]^{\frac{1}{\gamma}},\ m = 1, 2. \end{aligned}$$

Lemma 2 and inequalities (20) imply

$$\left| e^{-(2\pi n)^2 \int_0^t k_1(s)ds} - e^{-(2\pi n)^2 \int_0^t k_2(s)ds} \right| \leq \frac{(\alpha_1 - \alpha)^{\frac{1}{\gamma}}}{\beta^{\frac{1}{\gamma}} e} \|k_1 - k_2\|_{C[0,T]}.$$

Then, we obtain

$$\begin{aligned} |\alpha_{0,2}(t) - \alpha_{0,1}(t)| &\leq \frac{(\alpha_1 - \alpha)^{\frac{1}{\gamma}}}{\beta^{\frac{1}{\gamma}} e} \left( \frac{2}{\pi} \sum_{n=1}^{\infty} \frac{1}{n} \varphi_{2n} \right) \|k_1 - k_2\|_{C[0,T]}, \\ |\alpha_{1,2}(t) - \alpha_{1,1}(t)| &\leq \frac{(\alpha_1 - \alpha)^{\frac{1}{\gamma}}}{\beta^{\frac{1}{\gamma}} e} \left( 16\pi T \sum_{n=1}^{\infty} n\varphi_{2n} - 4 \sum_{n=1}^{\infty} \varphi_{2n-1} \right) \|k_1 - k_2\|_{C[0,T]}. \end{aligned}$$

From these inequalities and (21), we obtain

$$\max_{0 \leq t \leq T} |F[p_1(t)] - F[p_2(t)]| \leq \frac{(\alpha_1 - \alpha)^{\frac{1}{\gamma}}}{\beta^{\frac{1}{\gamma}}} \delta \|k_1 - k_2\|_{C[0,T]}, \tag{22}$$

where

$$\delta = \frac{2}{\pi e} \frac{(8\pi^2 T \alpha_1 + 1) \sum_{n=1}^{\infty} n\varphi_{2n} - 2\pi\alpha_1 \sum_{n=1}^{\infty} \varphi_{2n-1}}{-2\varphi_0 - 4\varphi_1}. \tag{23}$$

By using the mean value theorem and (20), it is easy to show that

$$|k_1(t) - k_2(t)| \leq \frac{\beta^{\frac{1}{\gamma}}}{\gamma (\alpha_0 - \alpha)^{1+\frac{1}{\gamma}}} |p_1(t) - p_2(t)|. \tag{24}$$

Thus, from (22) and (24) we obtain

$$\|F[p_1] - F[p_2]\|_{C[0,T]} \leq \frac{\delta}{(\alpha_0 - \alpha)} \frac{1}{\gamma} \left( \frac{\alpha_1 - \alpha}{\alpha_0 - \alpha} \right)^{1/\gamma} \|p_1 - p_2\|_{C[0,T]}.$$

Let us fix a sufficiently large number $\gamma_0 > 0$ such that

$$K := \frac{\delta}{(\alpha_0 - \alpha)} \frac{1}{\gamma_0} \left( \frac{\alpha_1 - \alpha}{\alpha_0 - \alpha} \right)^{1/\gamma_0} \leq 1. \tag{25}$$

Thus, in the case $\gamma > \gamma_0$, equation (16) has a unique solution $k(t) \in C_{\alpha_0,\alpha_1}[0,T]$, by the Banach fixed point theorem.

We therefore obtain a unique positive function $k(t)$, continuous on $[0,T]$, which, together with the solution of the problem (1)–(4) given by the Fourier series (15), form the unique solution of the inverse problem (1)–(5). This concludes the proof of the theorem. □

## 3.2 Continuous Dependence Upon the Data

The following result on continuously dependence on the data of the solution of the inverse problem (1)–(5) holds.

**Theorem 2.** *Consider the (input) data in the form of $\Phi = \{\varphi, E\}$ which satisfy the assumptions of Theorem 1 with*

$$2\varphi_0 - E_{\max} \geq N_1 > 0, \quad \varphi_0 + 2\varphi_1 \leq -N_2 < 0 \tag{26}$$

*and let*

$$\|\varphi\|_{C^3[0,1]} \leq N_3, \quad \|E\|_{C[0,T]} \leq N_4 \tag{27}$$

*for some positive numbers $N_1, N_2, N_3$ and $N_4$. Then the solution $(k(t), u(x,t))$ of the inverse problem (1)–(5) depends continuously upon the data for sufficiently small $\alpha$ and large $\gamma$.*

*Proof.* Let $\Phi = \{\varphi,\ E\}$ and $\overline{\Phi} = \left\{\overline{\varphi},\ \overline{E}\right\}$ be two sets of the data, which satisfy the conditions of Theorem 1. Let us denote $\|\Phi\| := \|\varphi\|_{C^3[0,1]} + \|E\|_{C[0,T]}$.

Let $(k,u)$ and $\left(\overline{k}, \overline{u}\right)$ be solutions of the inverse problem (1)–(5) corresponding to the data $\Phi$ and $\overline{\Phi}$, respectively. According to (17),

$$p(t) = \frac{2\varphi_0 + \frac{2}{\pi} \sum\limits_{n=1}^{\infty} \frac{1}{n} \varphi_{2n} e^{-(2\pi n)^2 \int\limits_0^t k(s)ds} - E(t)}{-2\varphi_0 + 4 \sum\limits_{n=1}^{\infty} \left[ 4\pi n \varphi_{2n} t - \varphi_{2n-1} \right] e^{-(2\pi n)^2 \int\limits_0^t k(s)ds}}, \quad k(t) = \left[ \frac{\beta}{p(t) - \alpha} \right]^{\frac{1}{\gamma}},$$

$$\overline{p}(t) = \frac{2\bar{\varphi}_0 + \frac{2}{\pi} \sum\limits_{n=1}^{\infty} \frac{1}{n} \bar{\varphi}_{2n} e^{-(2\pi n)^2 \int\limits_0^t \bar{k}(s)ds} - \bar{E}(t)}{-2\bar{\varphi}_0 + 4 \sum\limits_{n=1}^{\infty} \left[ 4\pi n \bar{\varphi}_{2n} t - \bar{\varphi}_{2n-1} \right] e^{-(2\pi n)^2 \int\limits_0^t \bar{k}(s)ds}}, \quad \bar{k}(t) = \left[ \frac{\beta}{\bar{p}(t) - \alpha} \right]^{\frac{1}{\gamma}}.$$

First, let us estimate the difference $p-\bar{p}$. Using (12), (13) and (27), we obtain

$$\begin{aligned}
\left|\sum_{n=1}^{\infty}\frac{1}{n}\varphi_{2n}e^{-(2\pi n)^2\int_0^t k(s)ds}\right| &\leq c\left\|\varphi\right\|_{C^3[0,1]}\leq cN_3,\\
\left|\sum_{n=1}^{\infty}\left(4\pi n\varphi_{2n}t-\varphi_{2n-1}\right)e^{-(2\pi n)^2\int_0^t k(s)ds}\right| &\leq 4\pi c(1+T)N_3,
\end{aligned}$$

$$\begin{aligned}
&\left|\sum_{n=1}^{\infty}\frac{1}{n}\varphi_{2n}e^{-(2\pi n)^2\int_0^t k(s)ds}-\sum_{n=1}^{\infty}\frac{1}{n}\bar{\varphi}_{2n}e^{-(2\pi n)^2\int_0^t \bar{k}(s)ds}\right|\\
\leq\ & M_1\left\|\varphi-\overline{\varphi}\right\|_{C^3[0,1]}+M_2\left\|k-\overline{k}\right\|_{C[0,T]},\\
&\left|\sum_{n=1}^{\infty}\left(4\pi n\varphi_{2n}t-\varphi_{2n-1}\right)e^{-(2\pi n)^2\int_0^t k(s)ds}-\sum_{n=1}^{\infty}\left(4\pi n\bar{\varphi}_{2n}t-\bar{\varphi}_{2n-1}\right)e^{-(2\pi n)^2\int_0^t \bar{k}(s)ds}\right|\\
\leq\ & M_3\left\|\varphi-\overline{\varphi}\right\|_{C^3[0,1]}+M_4\left\|k-\overline{k}\right\|_{C[0,T]},
\end{aligned}$$

where $M_k$, $k=\overline{1,4}$ are some positive constants. By using these inequalities, simple manipulations yield the estimate

$$|p(t)-\overline{p}(t)|\leq\frac{M_5\left\|\varphi-\overline{\varphi}\right\|_{C^3[0,1]}+M_6\left\|k-\overline{k}\right\|_{C[0,T]}+M_7\left\|E-\overline{E}\right\|_{C[0,T]}}{4N_2^2},\tag{28}$$

where $M_k$, $k=\overline{5,7}$ are some constants that are determined by $c_1,c_2$ and $N_k$, $k=\overline{1,4}$.

It is known from (24) that, for $\alpha<\alpha_0$,

$$\left|k(t)-\bar{k}(t)\right|\leq\frac{\beta^{\frac{1}{\gamma}}}{\gamma\left(\alpha_0-\alpha\right)^{1+\frac{1}{\gamma}}}\left|p(t)-\bar{p}(t)\right|,\tag{29}$$

with $\alpha_0\geq\frac{2\varphi_0-E_{\max}}{M_8\|\varphi\|_{C^3[0,1]}}\geq\frac{N_1}{M_8N_3}$, for some positive constant $M_8$. If $\alpha$ is sufficiently small such that $\alpha<\frac{N_1}{M_8N_3}$, using (29) in (28) we obtain

$$\left(1-M_9\right)\left\|p-\overline{p}\right\|_{C[0,T]}\leq M_{10}\left(\left\|\varphi-\overline{\varphi}\right\|_{C^3[0,1]}+\left\|E-\overline{E}\right\|_{C[0,T]}\right),\tag{30}$$

for some positive constants $M_{10}$ and $M_9:=\frac{M_6}{4N_2^2}\frac{\beta^{\frac{1}{\gamma}}}{\gamma\left(\frac{N_1}{M_8N_3}-\alpha\right)^{1+\frac{1}{\gamma}}}$.

The inequality $M_9<1$ holds for sufficiently large $\gamma$. This means that $p$ continuously depends upon the data. Then, the equality $k(t)=\left[\frac{\beta}{p(t)-\alpha}\right]^{1/\gamma}$ implies the continuous dependence of $k$ upon the data. Similarly, we can prove that $u$, which is given in (15), depends continuously upon the data. This concludes the proof of the theorem. □

# 4 Numerical Solution of Direct Problem

In this section, we consider the direct initial boundary value problem given by equations (1)–(4) when $k(t)$ is given and the dependent variable $u(x,t)$ is the solution to be determined. We use the finite-difference method (FDM) with a Crank-Nicolson scheme, [13], which is unconditionally stable and second-order accurate in space and time.

The discrete form of the direct problem is as follows. Take two positive integer $M$ and $N$ and let $\Delta x = 1/M$ and $\Delta t = T/N$ be step lengths in space and time directions, respectively. We subdivided the domain $Q_T = (0,1) \times (0,T)$ into $M \times N$ subintervals of equally step length. At the node $(i,j)$ we denote $u_{i,j} = u(x_i, t_j)$, $k(t_j) = k_j$, where $x_i = i\Delta x$, $t_j = j\Delta t$, for $i = \overline{0,M}$, $j = \overline{0,N}$. Considering the general partial differential equation

$$u_t = G(x, t, u_{xx}), \tag{31}$$

equation (31) subject to (2)–(4) can approximated as:

$$\frac{u_{i,j+1} - u_{i,j}}{\Delta t} = \frac{1}{2}\left(G_{i,j} + G_{i,j+1}\right), \quad i = \overline{1,M},\ j = \overline{0,(N-1)}, \tag{32}$$

$$u_{i,0} = \varphi(x_i), \quad i = \overline{0,M}, \tag{33}$$

$$u_{0,j} = u_{M,j}, \quad j = \overline{0,N}, \tag{34}$$

$$u_{M+1,j} = u_{M-1,j}, \quad j = \overline{0,N}, \tag{35}$$

where

$$G_{i,j} = G\left(x_i, t_j, \frac{u_{i+1,j} - 2u_{i,j} + u_{i-1,j}}{(\Delta x)^2}\right), \quad i = \overline{1,M},\ j = \overline{0,(N-1)}. \tag{36}$$

For our problem, equation (1) can be discretised in the form of (32) as

$$\begin{aligned} -A_{j+1}u_{i-1,j+1} + (1 + B_{j+1})u_{i,j+1} - A_{j+1}u_{i+1,j+1} = \\ A_j u_{i-1,j} + (1 - B_j)u_{i,j} + A_j u_{i+1,j}, \end{aligned} \tag{37}$$

for $i = \overline{1,M}$, $j = \overline{0,(N-1)}$, where

$$A_j = \frac{(\Delta t)k_j}{2(\Delta x)^2}, \qquad B_j = \frac{(\Delta t)k_j}{(\Delta x)^2}.$$

At each time step $t_{j+1}$, for $j = \overline{0,(N-1)}$, using the periodic boundary conditions (34), the above difference equation can be reformulated as a $M \times M$ system of linear equations of the form,

$$D\mathbf{u}_{j+1} = \mathrm{E}\mathbf{u}_j, \tag{38}$$

where

$$\mathbf{u}_{j+1} = (u_{1,j+1}, u_{2,j+1}, ..., u_{M,j+1})^{\mathrm{T}},$$

$$D = \begin{pmatrix} 1+B_{j+1} & -A_{j+1} & 0 & \cdots & 0 & 0 & -A_{j+1} \\ -A_{j+1} & 1+B_{j+1} & -A_{j+1} & \cdots & 0 & 0 & 0 \\ \vdots & \vdots & \vdots & \ddots & \vdots & \vdots & \vdots \\ 0 & 0 & 0 & \cdots & -A_{j+1} & 1+B_{j+1} & -A_{j+1} \\ 0 & 0 & 0 & \cdots & 0 & -2A_{j+1} & 1+B_{j+1} \end{pmatrix}_{M\times M},$$

and

$$E = \begin{pmatrix} 1-B_j & A_j & 0 & \cdots & 0 & 0 & A_j \\ A_j & 1-B_j & A_j & \cdots & 0 & 0 & 0 \\ \vdots & \vdots & \vdots & \ddots & \vdots & \vdots & \vdots \\ 0 & 0 & 0 & \cdots & A_j & 1-B_j & A_j \\ 0 & 0 & 0 & \cdots & 0 & 2A_j & 1-B_j \end{pmatrix}_{M\times M}.$$

## 4.1 Example

As an example, consider the direct problem (1)–(4) with $T = 1$ and

$$k(t) = \frac{1+t}{2\pi^2}, \quad u(x,0) = \varphi(x) = -\cos(2\pi x). \tag{39}$$

The exact solution is given by

$$u(x,t) = -\cos(2\pi x)e^{-t^2-2t}. \tag{40}$$

The required output (5) is

$$E(t) = p(t)u(0,t) + \int_0^1 u(x,t)dx = -\left(\alpha + \beta\left(\frac{1+t}{2\pi^2}\right)^{-\gamma}\right)e^{-t^2-2t}. \tag{41}$$

The numerical and exact solutions for $u(x,t)$ at the interior points are shown in Figure 1 and also the absolute error between them is included. One can notice that an excellent agreement is obtained. Figure 2 shows the numerical solution in comparison with the exact one for $E(t)$ for $\alpha = \beta = \gamma = 1$. The numerical values for $E$ have been calculated using equation (34) and the trapezoidal rule approximation to the integral in (41) to result in the formula

$$E(t_j) = p(t_j)u_{0,j} + \frac{1}{M}\sum_{i=0}^{M-1} u_{i,j}, \quad j = \overline{0,N}. \tag{42}$$

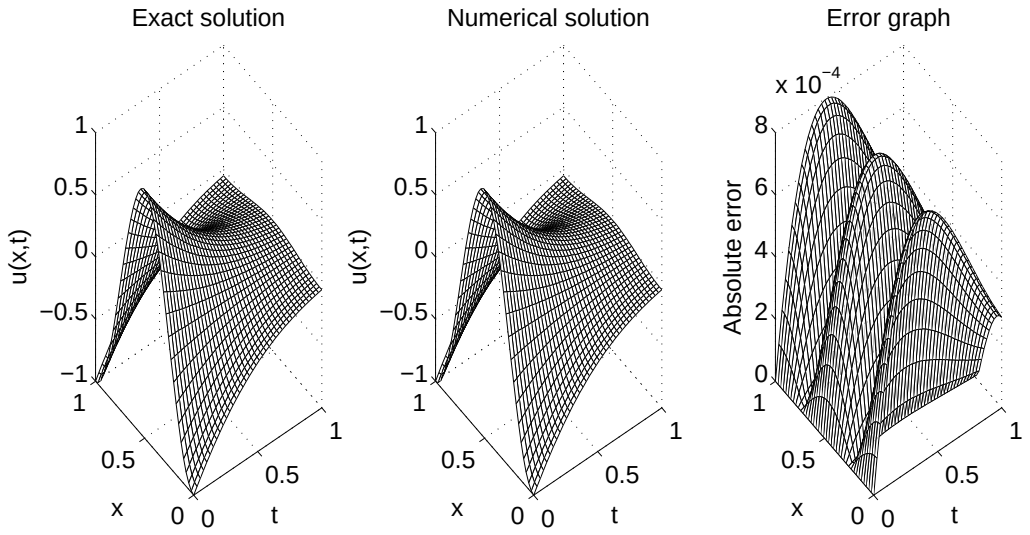


Figure 1: Exact and numerical solutions for $u(x,t)$ and the absolute error for the direct problem obtained with $M = N = 40$.

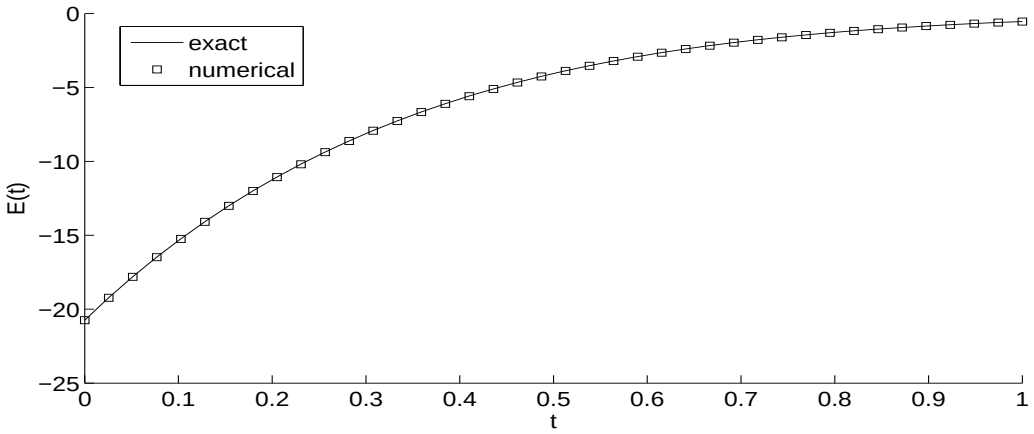


Figure 2: Exact and numerical solutions for $E(t)$ with $\alpha = \beta = \gamma = 1$ for the direct problem obtained with $M = N = 40$.

# 5 Numerical Solution of Inverse Problem

We wish to obtain stable and accurate reconstructions of the time-dependent thermal conductivity $k(t)$ and the temperature $u(x,t)$ satisfying the equations (1)–(5). We reduce the inverse problem to a nonlinear minimization of the least-squares objective function

$$F(k) := \left\| u(0,t)(\alpha + \beta k^{-\gamma}(t)) + \int_0^1 u(x,t)dx - E(t) \right\|^2_{L^2[0,T]}. \tag{43}$$

The discretised form of (43) is

$$F(\underline{k}) = \sum_{j=1}^{N} \left[ u(0,t_j)(\alpha + \beta k_j^{-\gamma}) + \frac{1}{M} \sum_{i=0}^{M-1} u_{i,j} - E(t_j) \right]^2, \tag{44}$$

where $\underline{k} = (k_j)_{j=\overline{1,N}}$, the values $u_{i,j}$ are computed from (38) and, for simplicity, we have dropped the time-step multiplier $T/N$. It is worth mentioning that if the compatibility condition $u(0,0) = \varphi(0)$ is satisfied then (5) applied at $t = 0$, yields

$$k(0) = \left( \frac{\beta\varphi(0)}{E(0) - \int_0^1 \varphi(x)dx - \alpha\varphi(0)} \right)^{1/\gamma}. \tag{45}$$

The minimization of the objective functional (44), subjected to the physical simple bound constraints $\underline{k} > \underline{0}$ is accomplished using the MATLAB optimization toolbox routine *lsqnonlin*, which does not require supplying (by the user) the gradient of the objective function, [11]. Furthermore, within *lsqnonlin* we use the Trust-Region algorithm which is based on the interior-reflective Newton method, [2]. Each iteration involves a large linear system of equations whose solution, based on a preconditioned conjugate gradient method, allows a regular and sufficiently smooth decrease of the objective functional (44), [1].

In the numerical computation, we take the parameters of the routine *lsqnonlin* as follows:

- Number of variables $M = N = 40$.

- Maximum number of iterations = $10^2 \times$ (number of variables).
- Maximum number of objective function evaluations = $10^3 \times$ (number of variables).
- Solution tolerance = $10^{-10}$.
- Object function tolerance = $10^{-10}$.
- Nonlinear constraint tolerance = $10^{-6}$.

The inverse problem (1)–(5) is solved subject to both exact and noisy measurements (5). The noisy data is numerically simulated as

$$E^{\epsilon}(t_j) = E(t_j) + \epsilon_j, \quad j = \overline{1, N}, \tag{46}$$

where $\epsilon_j$ are random variables generated from a Gaussian normal distribution with mean zero and standard deviation $\sigma$ given by

$$\sigma = \rho \times \max_{t \in [0,T]} |E(t)|, \tag{47}$$

where $\rho$ represents the percentage of noise. We use the MATLAB function *normrnd* to generate the random variables $\underline{\epsilon} = (\epsilon_j)_{j=\overline{1,N}}$ as follows:

$$\underline{\epsilon} = normrnd(0, \sigma, N). \tag{48}$$

The total amount of noise $\epsilon$ is given by

$$\epsilon = \left|\underline{\epsilon}\right| = \sqrt{\sum_{j=1}^{N} (E^{\epsilon}(t_j) - E(t_j))^2}. \tag{49}$$

In the case of noisy data (46), we replace $E(t_j)$ by $E^{\epsilon}(t_j)$ in (44).

# 6 Numerical Results and Discussion

In this section, we present and discuss a few test examples in order to illustrate the accuracy, stability and robustness of the numerical scheme based on the FDM combined with the minimization of the least-squares functional (44), as described in Section 5.

## 6.1 Example 1

In this example, we consider the inverse problem (1)-(5) with $T = 1$ and the input data

$$u(x, 0) = \varphi(x) = -\frac{\cos(2\pi x)}{e}, \quad E(t) = -\left(1 + 8\pi^2\sqrt{1+t}\right)\exp(-\sqrt{1+t}), \tag{50}$$

and $\alpha = \beta = \gamma = 1$. One can easily check that $E(t) \in C[0,1]$ and that $C^3[0,1] \ni \varphi(x)$ satisfies the conditions in (14a). Moreover, using (11) we have

$$\begin{aligned}
\varphi_0 &= \int_0^1 \varphi(x) Y_0(x) dx = -\frac{1}{e}\int_0^1 x\cos(2\pi x) dx = 0,\\
\varphi_1 &= \int_0^1 \varphi(x) Y_1(x) dx = -\frac{1}{e}\int_0^1 x^2\cos^2(2\pi x) dx = -\frac{1}{4e},\\
\varphi_{2k} &= \int_0^1 \varphi(x) Y_{2k}(x) dx = -\frac{1}{e}\int_0^1 \cos(2\pi x)\sin(2\pi k x) dx = 0, \quad k \geq 1\\
\varphi_{2k-1} &= \int_0^1 \varphi(x) Y_{2k-1}(x) dx = -\frac{1}{e}\int_0^1 x\cos(2\pi x)\cos(2\pi k x) dx = 0, \quad k \geq 2
\end{aligned}$$

and hence, one can easily check that the conditions in (14b) are also satisfied. We can also calculate from (18) and (23) that

$$\alpha_0 = \frac{E_{\max}}{4\varphi_1} \simeq 74.45, \quad \alpha_1 = \frac{E_{\min}}{4\varphi_1} \simeq 79.95, \quad \delta = \frac{\alpha_1}{e} \simeq 29.41, \tag{51}$$

where

$$\begin{aligned}
E_{\max} &= \max_{t\in[0,1]} E(t) = E(1) = -\frac{1+8\pi^2\sqrt{2}}{e^{\sqrt{2}}} \simeq -27.38,\\
E_{\min} &= \min_{t\in[0,1]} E(t) = E(1) = -\frac{1+8\pi^2}{e} \simeq -29.41.
\end{aligned}$$

Then the quantity $K$ in equation (25) is given by $K = \frac{0.4004}{\gamma_0} \times (1.0749)^{1/\gamma_0}$, and $K \leq 1$ if $\gamma_0 \geq 0.5$ for example. Anyway, our choice $\alpha = \gamma = 1$ satisfies $\alpha < \alpha_0 = 74.45$ and $\gamma > \gamma_0 = 0.5$ and hence according the Theorem 1 the solution of the inverse problem exits and is unique. In fact, it can easily be checked by direct substitution that the analytical solution is given by

$$k(t) = \frac{1}{8\pi^2\sqrt{1+t}}, \quad u(x,t) = -\cos(2\pi x)\exp(-\sqrt{1+t}). \tag{52}$$

We take the initial guess for the unknown thermal diffusivity $k(t)$ equal to the constant $k(0) = 1/(8\pi^2)$ which is known from expression (45).

First, we attempt to retrieve the unknown diffusivity $k(t)$ and the concentration/ temperature $u(x,t)$ for exact input data, i.e. $\rho = 0$, as well as for $\rho \in \{2\%, 20\%\}$ noisy data. The objective function (44) is plotted, as a function of the number of iterations, in Figure 3. From this figure, it can be seen that a very fast convergence is achieved in 4 to 8 iterations to reach a very low value of $O(10^{-25})$. The associated numerically obtained results for $k(t)$ and $u(x,t)$ are presented in Figures 4 and 5, respectively. From these figures it can be seen clearly that the agreement between the numerical results and the analytical solutions is excellent for exact data, i.e. $\rho = 0$, and is consistent with the errors in the input data for $\rho > 0$. The numerical solutions for $k(t)$ and $u(x,t)$ converge to their corresponding exact solutions in (52), as the percentage of noise $\rho$ decreases from 20% to 2% and then to zero. The nonlinear least-squares minimization (44) produces good and consistent reconstructions of the solution even for a large amount of noise such as 20%, when the total amount of noise computed by (49) is $\epsilon = 33.7$.

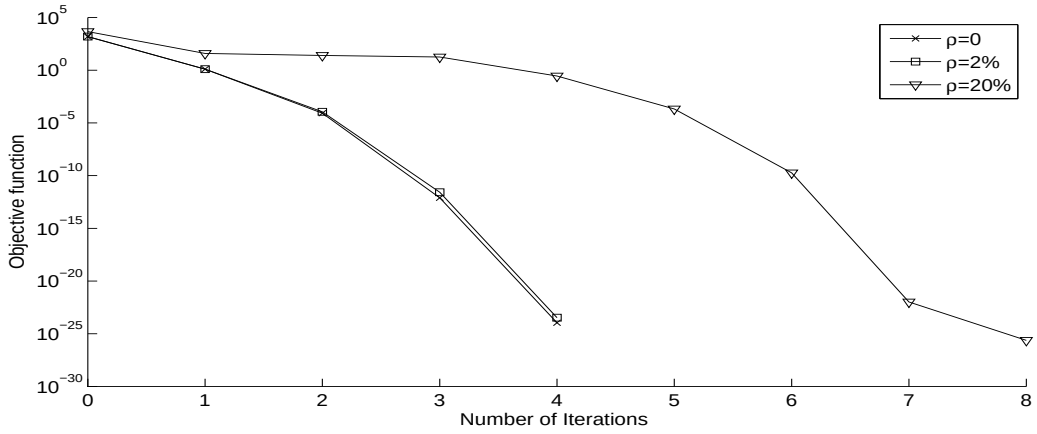


Figure 3: Objective function (44), for Example 1 with $\rho \in \{0, 2\%, 20\%\}$ noise.

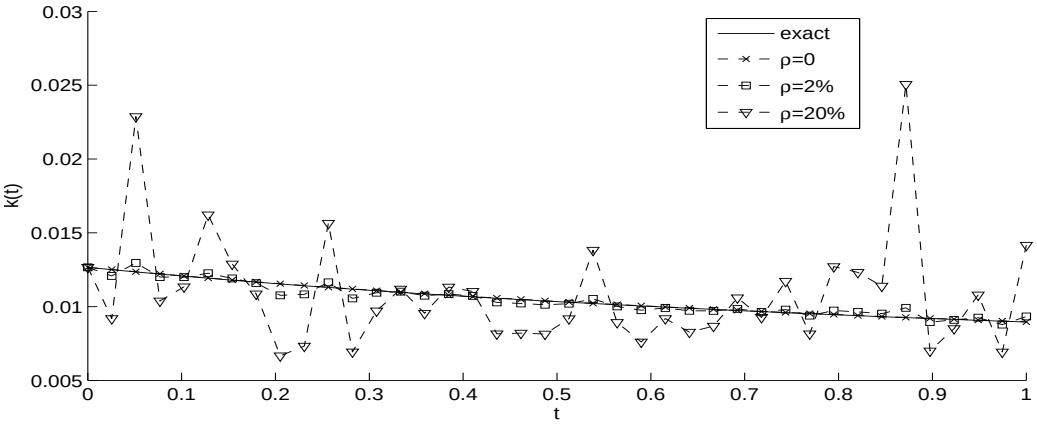


Figure 4: Exact and numerical solutions for $k(t)$, for Example 1 with $\rho \in \{0, 2\%, 20\%\}$ noise.

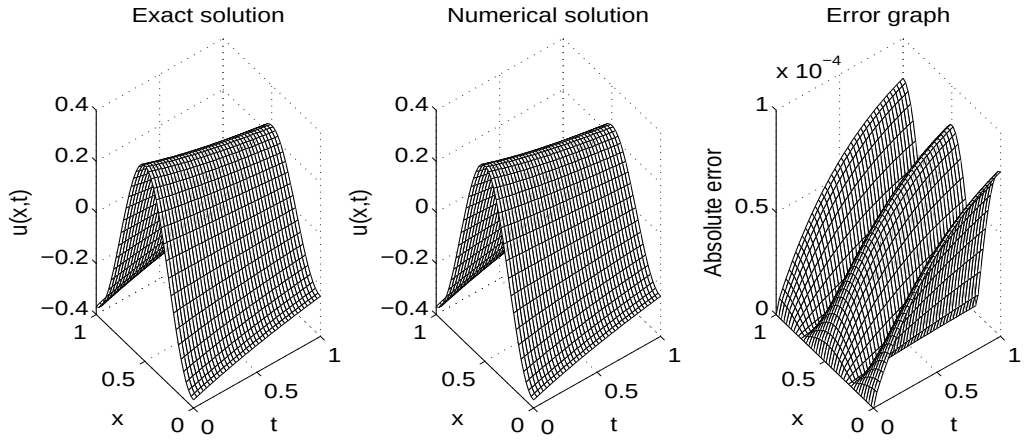


(a)

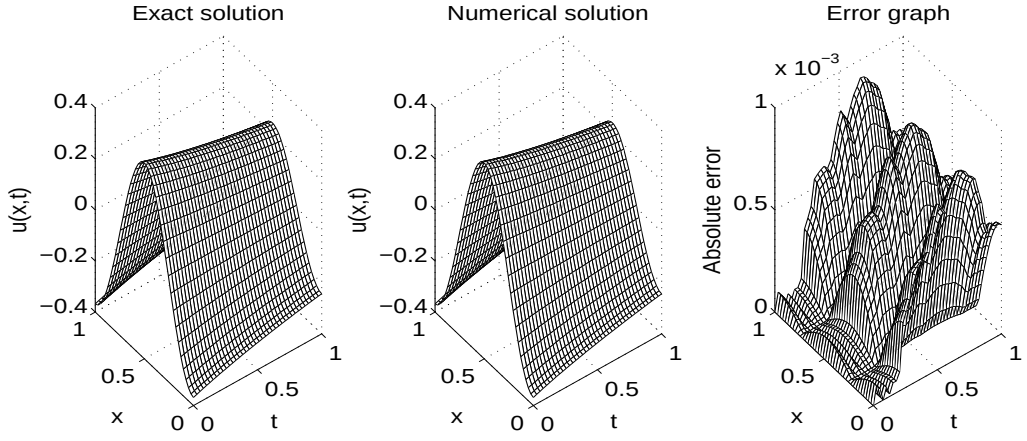


(b)

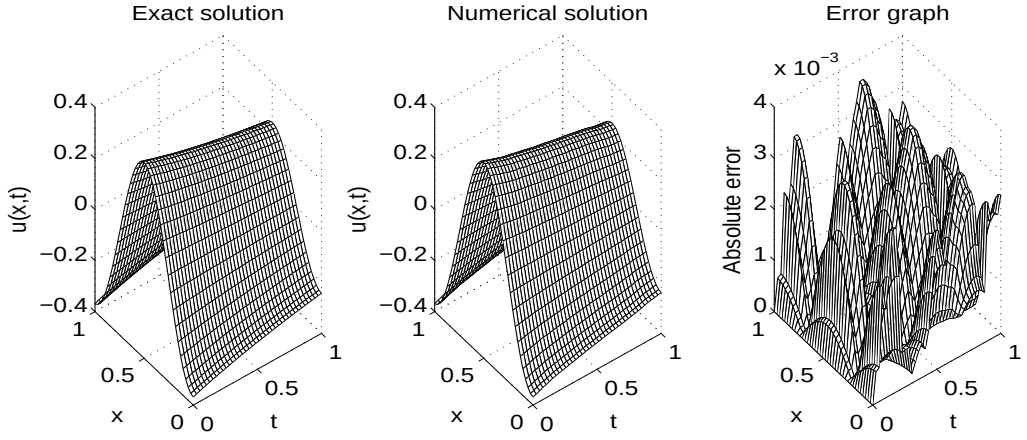


(c)

Figure 5: Exact and numerical solutions for $u(x,t)$, for Example 1 with (a) no noise, (b) $\rho = 2\%$ noise, and (c) $\rho = 20\%$ noise. The absolute error between them is also included.

## 6.2 Example 2

Consider the inverse problem (1)-(5) with $T = 1$ and the input data

$$u(x,0) = \varphi(x) = -\cos(2\pi x), \quad E(t) = -\left(1 + \left(\frac{1+t}{2\pi^2}\right)^{-1}\right) e^{-t^2-2t}, \tag{53}$$

and $\alpha = \beta = \gamma = 1$. As in Example 1, it is easy to check conditions (14a) and (14b) of Theorem 1 are satisfied. We also obtain that $\varphi_k = 0$ for all $k \in \mathbb{N} \setminus \{1\}$, $\varphi_1 = -1/4$, $E_{\min} = E(0) = -(1 + 2\pi^2) \simeq -20.73$, $E_{\max} = E(1) = -(1 + \pi^2)e^{-3} \simeq -0.516$, and $\alpha_0 = E_{\max}/(4\varphi_1) = 0.516$. As the condition $1 < \alpha < \alpha_0 = 0.516$ of Theorem 1 is not satisfied we can not conclude the unique solvability of the inverse problem. However, the solution at least exists and is given by

$$k(t) = \frac{1+t}{2\pi^2}, \quad u(x,t) = -\cos(2\pi x)\exp(-t^2 - 2t). \tag{54}$$

which can easily be verified by direct substitution.

The FDM numerical solution of the direct problem associated to this example has already been presented and discussed in subsection 4.1. The uniqueness of solution (54) is not guaranteed from theory, but numerically we can at least investigate the obtained results from various initial guesses for the unknown diffusivity vector $\underline{k}$ which initiate the minimization of the objective function (44). This will also test the robustness of the iterative method with respect to the independence on the initial guess. This investigation is illustrated in Figures 6, 7 and Table 1 for exact data with various initial guesses

$$k^0(t) \in \{1/(2\pi^2), 1, 2\}, \quad t \in [0,1]. \tag{55}$$

Note that from (54) the initial guess $k^0(t) = 1/(2\pi^2)$ corresponds to the value of $k(0)$, which can be assumed to be known from (45). In Table 1, the root mean square error $rmse$ value of $k$ is calculated as

$$rmse(k) = \sqrt{\frac{1}{N}\sum_{j=1}^{N}(k_j - k_{exact}(t_j))^2}. \tag{56}$$

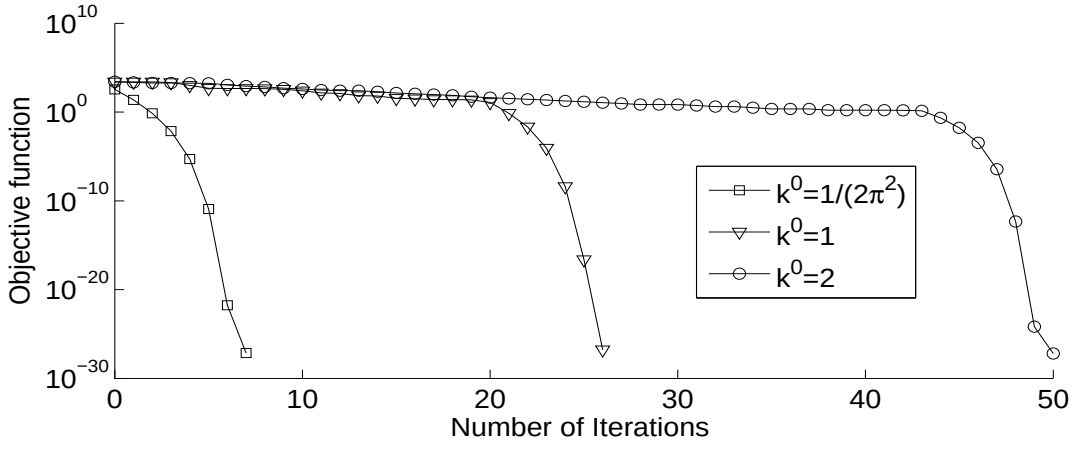


Figure 6: Objective function (44) for Example 2 with no noise and various initial guesses (55).

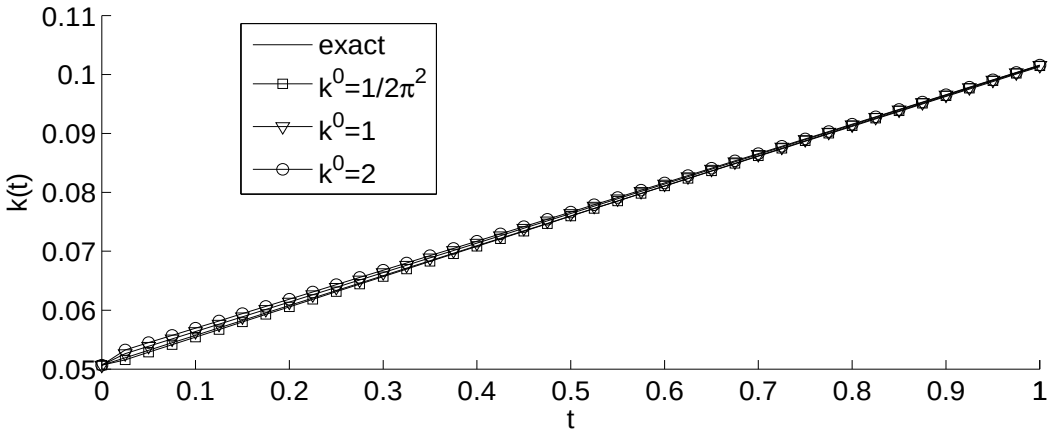


Figure 7: Exact and numerical solutions for $k(t)$, for Example 2 with no noise and various initial guesses (55).

Table 1: Number of iterations, number of function evaluations, value of the objective function (44) at final iteration, $rmse$ value (56) and the computational time, for Example 2 with no noise and various initial guesses (55).

| $\rho = 0$ | $k^0 = \frac{1}{2\pi^2}$ | $k^0 = 1$ | $k^0 = 2$ |
|---|---|---|---|
| No. of iterations | 7 | 26 | 50 |
| No. function evaluations | 336 | 1134 | 2142 |
| Value of objective function (44) at final iteration | 7.3E-28 | 1.7E-27 | 6.2E-28 |
| $rmse(k)$ | 1.6E-4 | 4.4E-4 | 7.6E-4 |
| Computational time | 31 sec | 105 sec | 198 sec |

From Figure 6 and Table 1 it can be seen that, as expected, the farther the initial guess is the more iterations and larger computational time are required to achieve convergence. However, for all initial guesses (55) the objective function (44) converges to the same minimum low value of $O(10^{-28})$. This shows robustness with respect to the independence on the initial guess. Furthermore, from Figure 7 and Table 1 it can be seen that the agreement between the exact and the numerically obtained solutions with various initial guesses is very good being of $O(10^{-4})$. There is also a slightly better accuracy for the closer initial guess $k^0 = 1/(2\pi^2)$ to the exact solution for $k(t)$ from (54).

In what follows, we take the initial guess for the unknown diffusivity $k(t)$ equal to the constant $k(0) = 1/(2\pi^2)$ which is known from expression (45).

Figure 8 shows the objective function (44) for $\rho \in \{0, 1\%\}$ as a function of the number of iterations. From this figure, it can be seen that the objective functional (44) decreases rapidly to a very low level of $O(10^{-28})$ in about 7 to 8 iterations. The corresponding exact and numerical solutions for $k(t)$ and $u(x,t)$ are presented in Figures 9 and 10, respectively. First, from Figures 5 and 10 it can be observed that accurate and stable solutions for $u(x,t)$ are obtained for both Examples 1 and 2. Secondly, for exact data, i.e. $\rho = 0$, the same conclusion regarding the excellent accuracy of the numerical solution for $k(t)$, as it was obtained for Example 1, can be drawn from Figure 4. However, for $\rho = 1\%$ noisy data some instability starts to manifest in Figure 9, as it also happened for Example 1 in Figure 4 for a much larger $\rho = 20\%$ amount of noise. We have also tried

to add some regularization term $\lambda\|k\|^2_{L^2[0,T]}$ with $\lambda > 0$ some regularization parameter to the nonlinear least-squares function (43), but the stability of the numerical solution did not improve.

We also mention that for higher amounts of noise, such as $\rho = 2\%$, the *lsqnonlin* minimization routine did not make significant progress after a large number of over 1000 iterations probably becoming trapped in a local minimum. One possible reason could be that the expressions for $k(t)$ given by equations (52) and (54) yield a stronger nonlinearity in $k^{-\gamma}(t)$ in (43) for Example 2 than for Example 1.

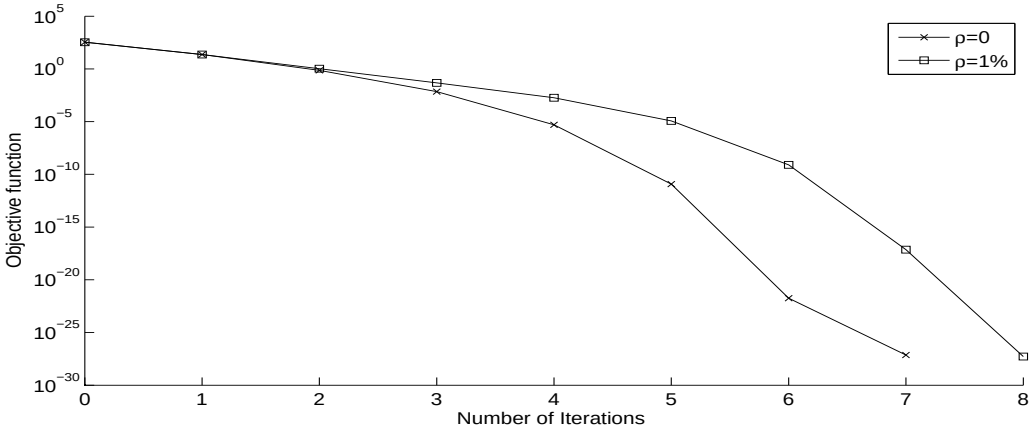


Figure 8: Objective function (44), for Example 2 with $\rho \in \{0, 1\%\}$ noise.

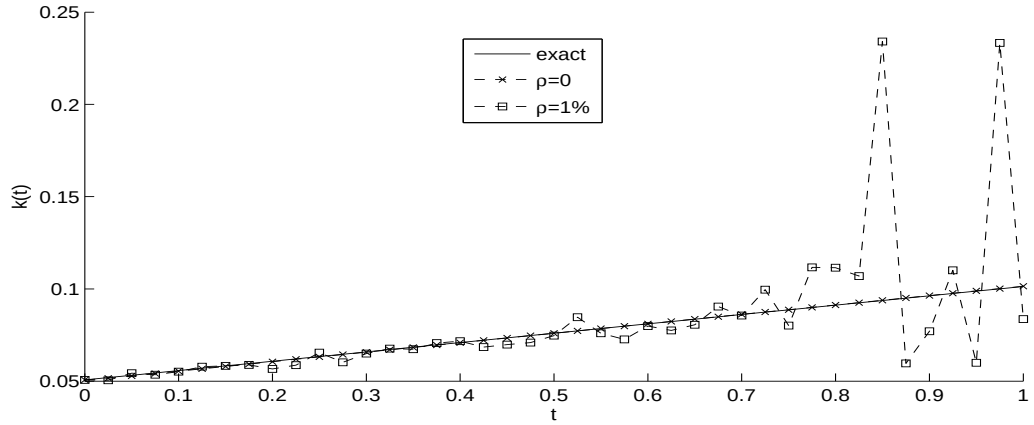


Figure 9: Exact and numerical solutions for $k(t)$, for Example 2 with $\rho \in \{0, 1\%\}$ noise.

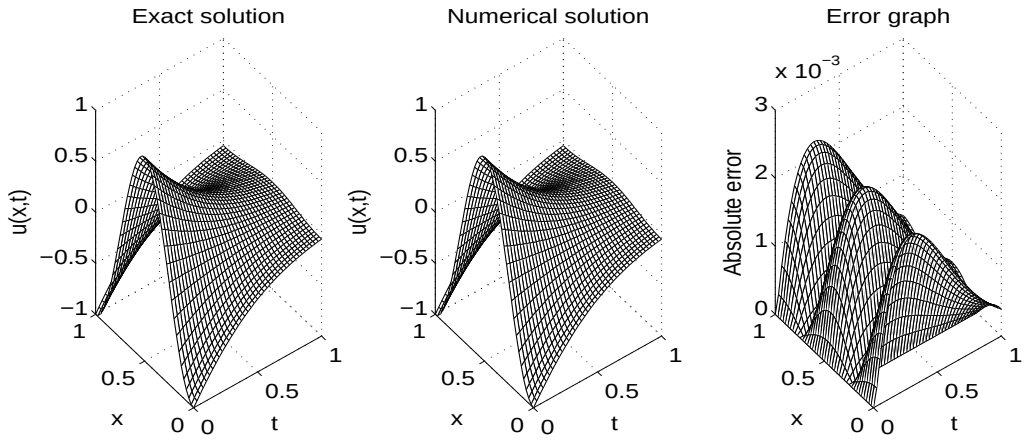


(a)

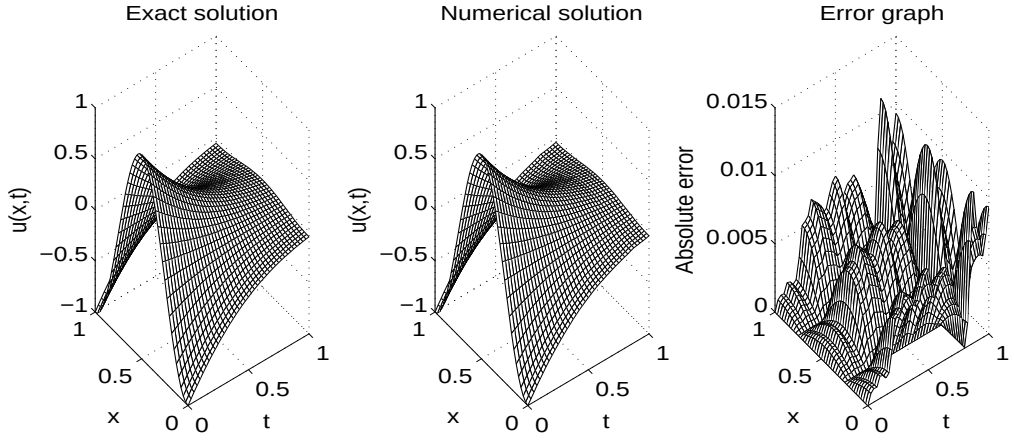


(b)

Figure 10: Exact and numerical solutions for $u(x,t)$, for Example 2 with (a) no noise, and (b) $\rho = 1\%$ noise. The absolute error between them is also included.

## 6.3 Example 3

The previous examples possessed analytical solutions available for the pair $(k(t), u(x,t))$, as given by equations (52) and (54). In this subsection, we investigate an example for which an explicit analytical solution for $u(x,t)$ is not available. We take the initial condition (2) given by

$$u(x,0) = \varphi(x) = \begin{cases} 0, & 0 \le x < 1/4, \\ \frac{1}{4} - x, & 1/4 < x \le 1/2, \\ x - \frac{3}{4}, & 1/2 < x < 3/4, \\ 0, & 3/4 < x \le 1. \end{cases} \tag{57}$$

This is severe test example because the initial data (57) is non-smooth function. Clearly, the initial data (57) violates some of the conditions of Theorem 1 which is not applicable for this example. However, we can make the inverse problem at least solvable by solving first the direct well-posed problem (1)–(4) with $\varphi(x)$ given by (57) and the diffusivity $k(t)$

given by

$$k(t) = \frac{1}{1+t}, \quad t \in [0,1], \tag{58}$$

in order to provide the data (5). This is performed numerically using FDM described in Section 4.

The numerical results for $E(t)$ (with $\alpha = \beta = \gamma = 1$) are shown in Figure 11, for various mesh sizes $M = N \in \{20, 40, 80\}$. From this figure it can be seen that that numerical solution is convergent as the FDM mesh sizes decreases. Also, there is only a small difference between the numerical results obtained with various mesh sizes showing that the independence on the mesh has been achieved. Consequently, we take the results for $E(t)$ simulated from solving the direct problem with $M = N = 80$ as our exact input data (5) in the inverse problem (1)–(5). In order to avoid committing an inverse crime, in the inverse problem the number of space intervals is taken as $M = 70$ (different than 80), whilst the number of time steps $N$ is kept the same 80.

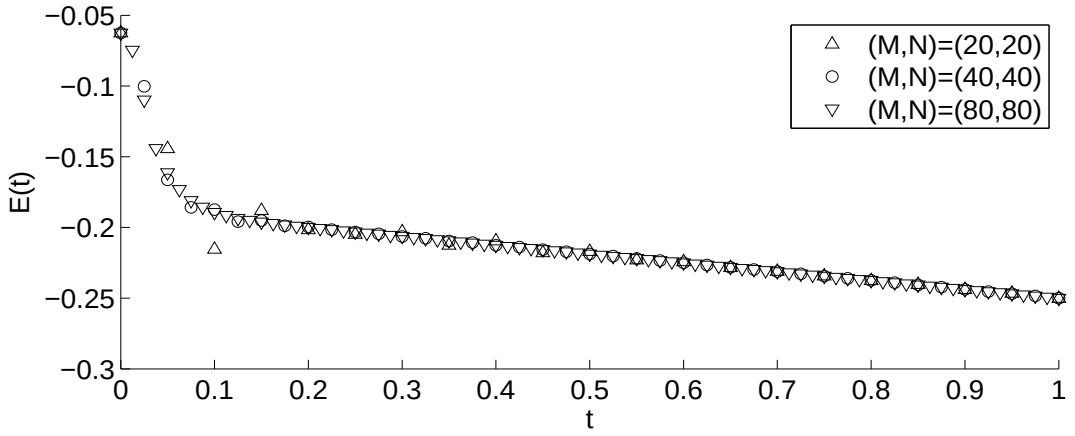


Figure 11: Numerical solution for $E(t)$, for the direct problem of Example 3 with various mesh sizes.

We take the initial guess $k^0 = 1$, noting at the same time that since $\varphi(0) = 0$ and $E(0) = -1/16$ equation (45) cannot be directly applied as it yields the non-determination $0/0$ division.

Figure 12 shows the objective function evolution (44), as a function of the number of iterations for no noise in the input data (5). From this figure it can be seen that a fast convergence is achieved in 20 iterations to reach a very low value of $O(10^{-12})$. The associated numerically obtained results for $k(t)$ are presented in Figure 13. From this figure it can be seen that the agreement between the numerical and the exact solutions is excellent, except for some slight unexpected discrepancy near $t = 0$.

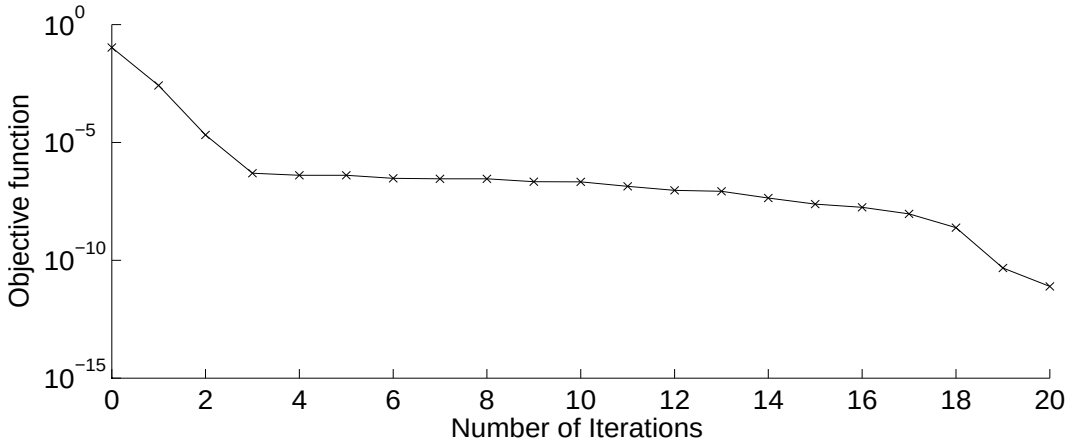


Figure 12: Objective function (44), for Example 3 with no noise.

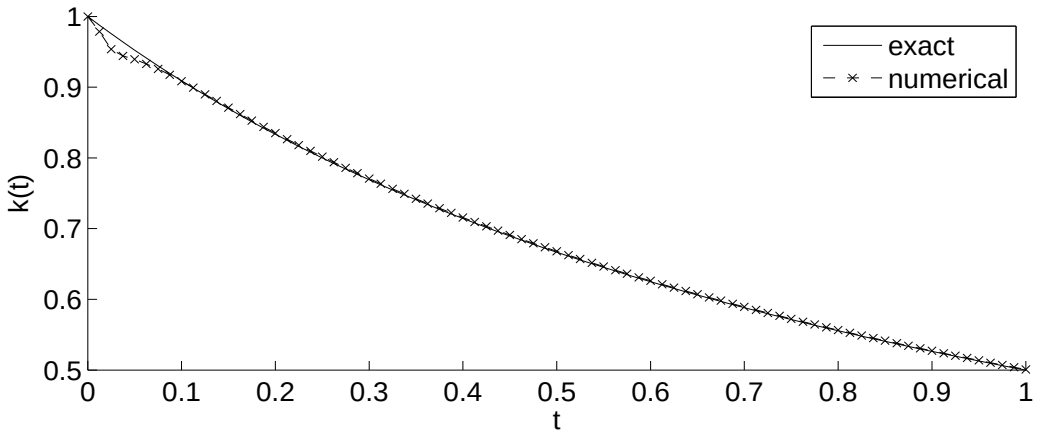


Figure 13: Exact and numerical solutions for $k(t)$, for Example 3 with no noise.

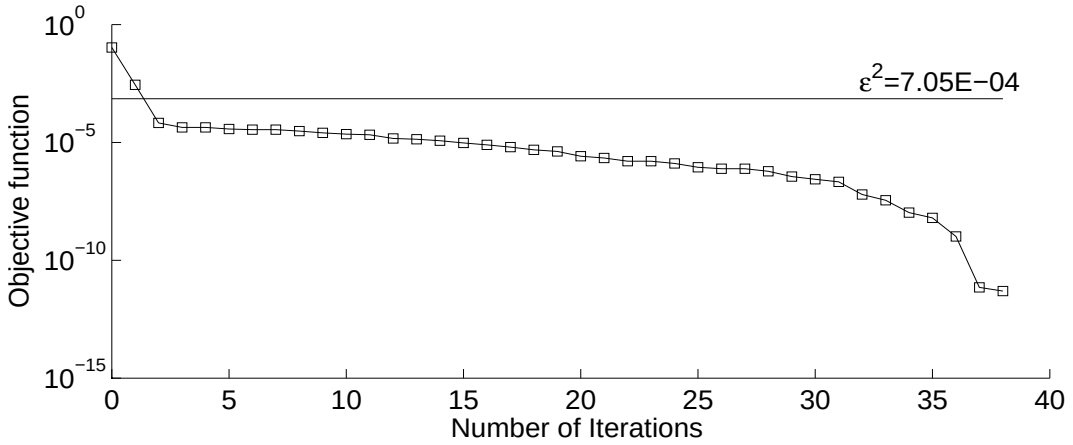


(a)

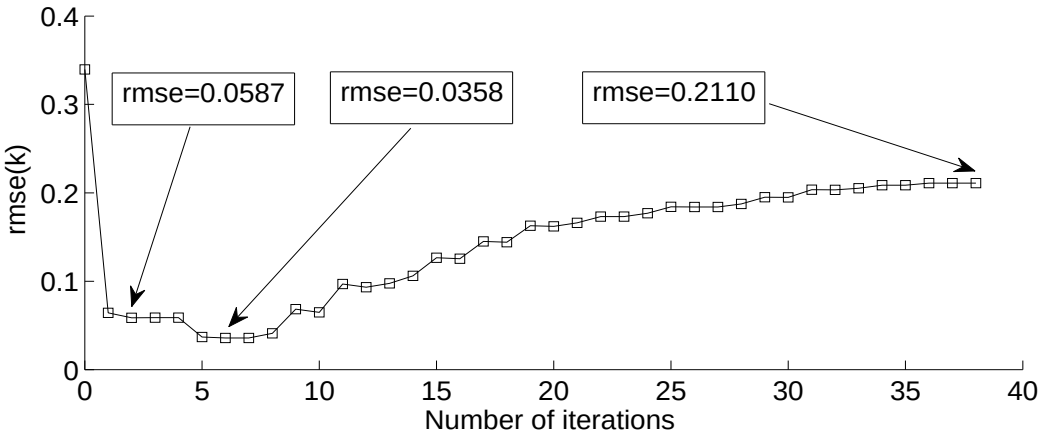


(b)

Figure 14: (a) Objective function (44) with horizontal noise threshold $\epsilon^2$=7.05E-4, and (b) the $rmse(k)$ values (56), for Example 3 with $\rho = 1\%$ noise.

Next we add $\rho = 1\%$ noise in the input data (5) numerically simulated as in (46). Figure 14(a) presents the objective function (44), as a function of the number of iterations together with the horizontal noise threshold $\epsilon^2$=7.05E-4 computed by (49). This threshold is useful when applying the discrepancy principle in order to stop the iteration process before the instability of solutions sets in. According to Figure 14(a) this criterion yields the iteration under $\text{iter}_{discr.} = 2$. Figure 14(a) also shows that the objective function (44) has converged after $\text{iter}_{conv.} = 38$. The $rmse(k)$ values (56) for unknown $k(t)$ are plotted, versus the number of iteration in Figure 14(b). Form this figure it can be remarked that the best retrieval occurs at $\text{iter}_{opt.} = 6$. For more clarity, the results of Figure 14 are summarised in Table 2 where the computational time is also included.

Finally, Figure 15 shows the exact solution (58) for $k(t)$ in comparison with the numerical solutions obtained after the iterations given by stopping criteria of Table 2. From this figure it can be seen that if the iterative process is not stopped, after $\text{iter}_{conv.} = 38$ we obtained a numerical approximation with $rmse(k) = 0.2110$ which moreover is not so accurate in the region $t \in [0, 0.2]$. However, if we stop the iterative process after $\text{iter}_{discr.} = 2$ iterations given by the discrepancy principle, which is graphically illustrated in Figure 14(a), then an accurate and stable numerical solution is achieved. Moreover, it yields an $rmse(k) = 0.0587$ which is close to the optimal one of $rmse(k) = 0.0358$. The

associated numerically obtained results for $k(t)$ plotted according to stopping criterion in Figure 15. From this figure it clear that the best retrieve for $k(t)$ is the (-□-) lines which meets the minimum $rmse$ value.

Table 2: The number of iterations, the $rmse(k)$ values (56) and the computational time based on several stopping criteria, for Example 3 with $p = 1\%$ noise.

| Criterion | No. of iterations | $rmse(k)$ | Computational time |
|---|---|---|---|
| to achieve convergence | $\text{iter}_{conv.}= 38$ | 0.2110 | 41 min |
| to achieve minimum $rmse(k)$ | $\text{iter}_{opt.}= 6$ | 0.0358 | 8 min |
| discrepancy principle | $\text{iter}_{discr.}= 2$ | 0.0587 | 3 min |

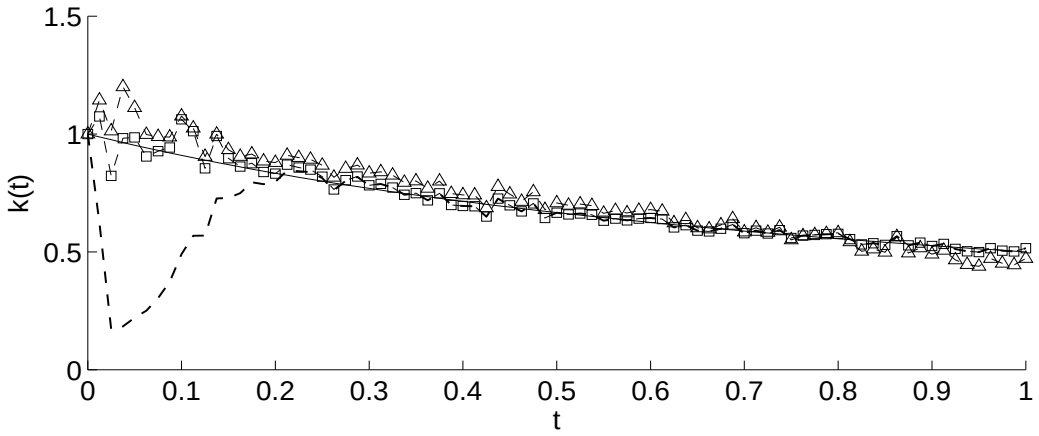


Figure 15: Exact (—) and the numerical solutions for $k(t)$ obtained after $\text{iter}_{conv.}$=38 (- - -), $\text{iter}_{opt.}$=6 (-□-), and $\text{iter}_{discr.}$=2 (-△-), for Example 3 with $\rho = 1\%$ noise.

# 7 Conclusions

An inverse nonlinear problem which requires identifying the time-dependent diffusivity with periodic boundary condition and non-local boundary measurement has been investigated. The unique solvability and continuous dependence upon the input data have all been proved. Numerically, the resulting inverse problem has been reformulated as a nonlinear least-squares optimization problem which has been solved using the MATLAB toolbox routine *lsqnonlin*. Numerical results show that accurate, robust and reasonably stable solutions have been obtained. This problem seems rather stable and hence, in general, no regularization was found necessary to be employed. However, for more severe examples which violate the sufficient conditions under which the well-posedness of the inverse problem hold, as expected, some regularization needs to be applied. For example, in Subsection 6.3 for the minimization of the *lsqnonlin* routine used, the discrepancy principle has been applied in order to terminate the iterative process before instability sets in and this in turn has produced stable and accurate numerical solution.

**Acknowledgments.** M.S. Hussein would like to thank the financial support received from the Higher Committee of Education Development in Iraq (HCEDiraq) for pursuing his Ph.D at the University of Leeds.

# References


[1] Baranger, T.N., Andrieux, S. and Rischette, R. (2014) Combained energy method and regularization to solve the Cauchy problem for the heat equation, *Inverse Problems in Science and Engineering*, **22**, 199-212.

[2] Conn, A., Gould, N. and Toint, P. (1987) *Trust Region Methods*, SIAM, Philadelphia.

[3] Ionkin, N.I. (1977) Solution of a boundary-value problem in heat conduction with a nonclassical boundary condition, *Differential Equations*, **13**, 204-211.

[4] Ismailov, M.I. and Kanca, F. (2011) An inverse coefficient problem for a parabolic equation in the case of nonlocal boundary and overdetermination conditions, *Mathematical Methods in the Applied Sciences*, **34**, 692–702.

[5] Ismailov, M.I. and Kanca, F. (2012) The inverse problem of finding the time-dependent diffusion coefficient of the heat equation from integral overdetermination data, *Inverse Problems in Science and Engineering*, **20**, 463–476.

[6] Ivanchov, M.I. (1994) Some inverse problems for the heat equation with nonlocal boundary conditions, *Ukrainian Mathematical Journal*, **45**, 1186-1192.

[7] Kanca, F. (2013) Inverse coefficient problem of the parabolic equation with periodic boundary and integral overdetermination conditions, *Abstract and Applied Analysis*, Vol. **2013**, Article ID 659804, (7 pages).

[8] Lesnic, D., Yousefi, S.A. and Ivanchov, M. (2013) Determination of a time-dependent diffusivity form nonlocal conditions, *Journal of Applied Mathematics and Computation*, **41**, 301-320.

[9] Muravei, L.A. and Petrov, V.M. (1987) Some problems of control of diffusion techological process, In: *Current Problems of Modelling and Control of System with Distributed Parameters*, Kiev, 42-43, (in Russian).

[10] Muravei, L.A. and Filinovskii, A.V. (1993) On a problem with nonlocal boundary condition for a parabolic equation, *Math. USSR Sbornik*, **74**, 219-249.

[11] Mathworks R2012 Documentation Optimization Toolbox-Least Squares (Model Fitting) Algorithms, available from www.mathworks.com/help/toolbox/optim/ug /brnoybu.html.

[12] Namazov, G.K. (1984) *Inverse Problems of the Theory of Equations of Mathematical Physics*, Baku, Azerbaijan, (in Russian).

[13] Smith, G.D. (1985) *Numerical Solution of Partial Differential Equations: Finite Difference Methods*, Clarendon Press, Oxford Applied Mathematics and Computing Science Series, Third Edition.

[14] Yousefi, S.A., Lesnic, D. and Barikbin, Z. (2012) Satisfier function in Ritz-Galerkin method for the identification of a time-dependent diffusivity, *Journal of Inverse and Ill-Posed Problems*, **20**, 701-722.